Probing Colossal Carbon Rings

Samuel J.P. Marlton,[†] Jack T. Buntine,[†] Patrick Watkins,[†] Chang Liu,[†] Ugo Jacovella,[‡] Eduardo Carrascosa,[¶] James N. Bull,[§] and Evan J. Bieske*[,†]

†*School of Chemistry, The University of Melbourne, Victoria, Australia 3010*

‡*Université Paris-Saclay, CNRS, Institut des Sciences Moléculaires d'Orsay, 91405 Orsay, France*

¶*Bruker Daltonics GmbH & Co. KG, Fahrenheitstrasse 4, 28359 Bremen, Germany*

§*School of Chemistry, Norwich Research Park, University of East Anglia, Norwich NR4 7TJ, United Kingdom*

E-mail: evanjb@unimelb.edu.au

Abstract

Carbon aggregates containing between 10 and 30 atoms preferentially arrange themselves as planar rings. To learn more about this exotic allotrope of carbon, electronic spectra are measured for even cyclo[n]carbon radical cations (C_{14}^+ – C_{36}^+) using two-color photodissociation action spectroscopy. To eliminate spectral contributions from other isomers, the target cyclo[n]carbon radical cations are isomer-selected using a drift tube ion mobility spectrometer prior to spectroscopic interrogation. The electronic spectra exhibit sharp transitions spanning the visible and near infrared spectral regions with the main absorption band shifting progressively to longer wavelength by ≈100 nm for every additional two carbon atoms. This behaviour is rationalised with a Hückel theory model describing the energies of the in-plane and out-of-plane π orbitals. Photoexcitation of smaller carbon rings leads preferentially to neutral C_3 and C_5 loss, whereas rings larger than C_{24}^+ tend to also decompose into two smaller rings, which,

when possible, have aromatic stability. Generally, the observed charged photofragments correspond to low energy fragment pairs, as predicted by density functional theory calculations (CAM-B3LYP-D3(BJ)/cc-pVDZ). Using action spectroscopy it is confirmed that C_{14}^+ and C_{18}^+ photofragments from C_{28}^+ rings have cyclic structures.

Introduction

Widespread acceptance that assemblies of carbon atoms adopt structures besides the familiar graphite and diamond allotropes followed the discovery of the C_{60} fullerene cluster and progressed with the synthesis of other fullerenes, carbon nanotubes and graphene.[1–3] Even before the discovery of fullerenes, it was proposed that the smaller carbon clusters exist predominately as linear chains, with rings (also known as cyclo[n]carbons) becoming the dominant isomer at n≈10 when the stabilization accompanying formation of an additional C-C bond outweighs the energetic penalty associated with bending the chain.[4,5] Charged carbon rings were probably first observed, without being recognised as such, by Hahn and coworkers in 1942 in mass spectra of ions produced in discharges between carbon electrodes,[6] and were later deduced to exist through gas-phase reactivity studies.[7,8] Subsequent ion mobility studies of $C_n^+$and C_n^- clusters formed by laser ablation of graphite provided compelling evidence for the existence of rings over the n=10–80 range, with rings being progressively supplanted as the dominant isomer by bi-rings (from C_{22}^+) and fullerenes (from C_{32}^+).[9–13] Examples of the co-existing ring, bi-ring and fullerene isomers are shown in Figure 1(a). The general chemical significance of cyclo[n]carbons is emphasized by the fact that they are formed through diverse routes, including by laser ablation of graphite, the decomposition of chlorinated polycyclic aromatic hydrocarbons (PAHs),[14] and the photoinduced dehydrogenation of PAHs.[15–17] Recently, in the culmination of longstanding efforts,[18,19] neutral C_{18} cyclo[n]carbons were synthesized on a surface and imaged individually using STM/AFM, demonstrating that the ring has polyynic rather than cumulenic bonding.[19]

Although there have been many theoretical investigations of cyclo[n]carbons,[2–5,20–23] fo-

cusing mainly on their structures and stabilities, experimental data against which the calculations can be compared and calibrated are rare. In this study we explore the photophysical and photochemical properties of charged, even cyclo[n]carbon cations up to C_{36}^+ in the gas phase, measuring electronic spectra, and investigating their decomposition following absorption of ultraviolet light. Earlier studies in which electronic spectra were measured for mass-selected rings up to C_{28}^+ tagged with N_2 molecules,[24] and with He atoms,[25] showed that even cyclo[n]carbon cations possess relatively sharp absorption bands over the visible (Vis) and near infrared (NIR) ranges, with a progressive linear shift of the strongest absorptions to longer wavelength by ≈100 nm for each additional two C atoms. Our preliminary investigations of the odd C_{2n+1}^+ rings indicate that the wavelengths of their electronic absorption bands do not fit with the trends established for the even C_{2n}^+ rings.

Here, we extend the earlier spectroscopic studies in several ways. First, we obtain electronic spectra of bare C_{2n}^+ carbon rings (C_{14}^+ – C_{36}^+) without attached tag atoms or molecules. Electronic spectra of the bare carbon rings along with previously reported C_{2n}^+-He_m and C_{2n}^+-$(N_2)_m$ spectra allow us to assess the shifts caused by attached He atoms and N_2 molecules, which are not known *a priori*. Wavelengths for the absorption peaks of the bare carbon clusters can be compared directly with astronomical data to decide whether cyclo[n]carbon cations exist in circumstellar and interstellar regions and whether their absorptions correspond to any diffuse interstellar bands (DIBs). Furthermore, spectra for larger carbon ring cations, C_{30}^+, C_{32}^+, C_{34}^+ and C_{36}^+, which have not been reported previously, allow us to investigate whether spectral patterns apparent for the smaller rings (up to C_{28}^+) persist for larger clusters. Probing the larger clusters (C_{28}^+ and above) presents challenges due to the coexistence of ring, bi-ring and fullerene isomers.[9–12,24] To address this issue, the carbon clusters are selected according to both their mass and their isomeric structure (using ion mobility) *prior* to spectroscopic interrogation, eliminating ambiguity in the size and structure of the species being probed.

Ideally, electronic spectra of the carbon ring cations would be understood with the aid

of electronic structure calculations. However, there is considerable debate over appropriate methods for describing even the ground electronic state properties of carbon rings,[5,20–23] so that reliably predicting wavelengths and intensities for electronic transitions of even smaller rings will be challenging, while reliable predictions for the larger rings are certainly currently not feasible. As a first step to understanding the electronic absorptions of carbon rings, we develop a simple model based on Hückel theory, describing the valence electrons occupying in-plane and out-of-plane π orbitals (Figure 1(b)). The model is consistent with the linear relationship between absorption wavelength and cluster size that was found to apply for even cyclo[n]carbon cations up to C_{28}^+.[24,25]

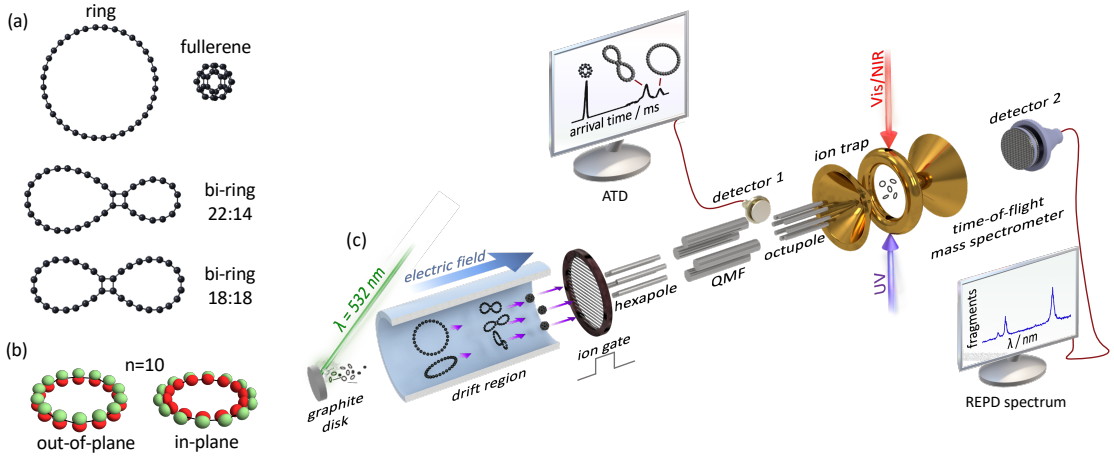

Figure 1: (a) Structures of C_{36}^+ isomers – ring, 18:18 and 22:14 bi-rings, and fullerene. (b) Lowest energy out-of-plane and in-plane π molecular orbitals for C_{10}. (c) Experimental strategy for spectroscopically probing mobility-selected carbon rings. Charged carbon clusters generated by pulsed laser ablation of a graphite disk are separated according to their collision cross sections with He buffer gas before passing through a quadrupole mass filter (QMF). An arrival time distribution (ATD), which shows peaks due to different isomers, can be measured by monitoring the ion signal at detector 1. For spectroscopy experiments, the target cyclo[n]carbon isomer population is selected by an electrostatic gate at the end of the drift tube, opened at an appropriate delay with respect to the ablation laser pulse, followed by mass selection with a quadrupole mass filter (QMF). The cyclo[n]carbon cations are introduced into a cryogenically cooled ion trap where they are spectroscopically probed using 2-colour resonance enhanced photodissociation (see Figure 2). An electronic spectrum is recorded by monitoring the photofragment intensity at detector 2 as a function of the wavelength of the Vis/NIR beam. A comprehensive description of the apparatus is given in refs. 24 and 26.

To learn more about the C_{14}^+– C_{36}^+ rings and to complement the spectroscopic studies, we have also investigated their photofragmentation behaviour. There have been several previous photodissociation studies of carbon clusters cations in the n=14–20 range (presumably rings), demonstrating that they mainly lose neutral C_3 or C_5 photofragments.[27–31] Photodissociation studies for larger rings in the C_{22}^+ – C_{36}^+ range are potentially complicated by the presence of coexisting isomers – rings and bi-rings for C_{22}^+ – C_{30}^+, and rings, bi-rings and fullerenes for C_{32}^+ – C_{36}^+. For example, Smalley and co-workers found that the photofragment distribution for C_{36}^+ depended on light intensity and on ion source conditions, which was taken as evidence for coexisting fullerene isomers (losing C_2 units) and non-fullerene isomers (giving C_n^+ photofragments in the n=14-22 range).[29] Later, Misaizu and coworkers addressed the isomeric ambiguity in photodissociation studies of C_{32}^+, C_{34}^+ and C_{36}^+, separating fullerene and non-fullerene isomers in an ion mobility drift cell before irradiating them with 266 nm light.[32] For each cluster size, the two isomer families produced distinct photoproduct ion distributions. However, in the ref. 29 and ref. 32 experiments, the non-fullerene population potentially contained ring and bi-ring isomers. To eliminate this ambiguity, we have adopted an isomer selective approach to probe C_{14}^+– C_{36}^+ rings. The resolution of our ion mobility stage is sufficient to cleanly separate the target rings from bi-rings and from fullerenes prior to photodissociation. To help interpret the observed photofragment distributions, relative energies of fragment pairs are calculated using density functional theory (DFT), allowing us to explore whether the preferred charged photofragments correspond to the lower energy fragment channels.

Despite the many measurements for photofragment distributions from charged carbon clusters, there have been no direct determinations of the fragments' structures (linear, ring, bi-ring or fullerene). In principle, the photofragment structures could be probed using a tandem ion mobility arrangement, with photoexcitation of the C_n^+ clusters after the first ion mobility stage, and separation of photofragment isomers in the second ion mobility stage.[33] Here we use an alternative spectroscopically-based strategy to investigate the structures of

the main C_{14}^+ and C_{18}^+ photofragments generated from C_{28}^+. The nascent photofragments are trapped, tagged with N_2 molecules, and irradiated with tunable radiation to record their characteristic electronic spectra.

Methods

Obtaining electronic or infrared spectra of larger cyclo[n]carbon cations entails dealing with complications associated with the presence of different isomers (rings, bi-rings and fullerenes), whose spectra may be entangled. To address this issue, we have developed an isomer-selective approach for measuring electronic spectra.[24,26,34] The experimental arrangement is shown schematically in Figure 1(c) and is described in more detail in refs. 24 and 26.

Carbon cluster cations were generated by laser ablation of a rotating graphite disk using the focused, frequency-doubled output of a pulsed Nd:YAG laser (λ=532 nm, 12 mJ/pulse, 100 Hz repetition rate). The ablation source is situated at the beginning of a drift tube ion mobility spectrometer which was used to separate the charged carbon clusters according to their drift time through He buffer gas ($P\approx$3 Torr). The target cyclo[n]carbon cations could be selected at the end of the drift tube using a pulsed electrostatic ion gate opened at an appropriately timed delay and duration. Following the ion gate, the charged clusters were collected by an RF ion funnel and passed through a 1 mm orifice into an RF hexapole ion guide (pressure typically 5×10^{-5} Torr), which was used to accumulate ions from 50 ablation laser pulses over 0.5 s. After emerging from the hexapole, the ions travelled through a quadrupole mass filter where they were mass selected and then passed through an octupole ion guide and into a cryogenically cooled quadrupole ion trap (QIT). Pulses of either He gas or He/N_2 100:1 gas mixture were injected at 2 Hz, with the gas pulse initiated 10–20 ms before arrival of the ion packet. The temperature of the trap ($T\approx$10 K) was measured using a Lakeshore DT-670 silicon diode. The actual temperature of the ions in the QIT is likely to be slightly higher than the trap temperature due to RF heating.

Electronic spectra of the C_{2n}^+ (n=7-18) clusters were obtained by 2-colour resonance enhanced photodissociation or through 1-colour resonance enhanced photodissociation of C_{2n}^+-$(N_2)_m$ complexes. Alternate packets of ions in the QIT were exposed to pulses of unfocused, wavelength-tunable light from an optical parametric oscillator (OPO, EKSPLA NT342B, $\leq$1 mJ/cm^2/pulse, 6 ns pulse width, bandwidth$\approx$4 cm^{-1}). Each tunable wavelength pulse was followed 10 ns later by a pulse of fixed wavelength UV light (OPO, EKSPLA NT342B, $\leq$1 mJ/cm^2/pulse, 6 ns pulse width, bandwidth$\approx$8 cm^{-1}), which served to dissociate the excited clusters. For clusters up to C_{26}^+, charged fragments corresponding to C_3 or C_5 loss were monitored, whereas for C_{28}^+ and larger clusters, C_{14}^+ or C_{18}^+ photofragments were monitored. The wavelength and power of the UV beam were adjusted to maximize the resonance enhanced photodissociation signal from the first tunable light pulse while minimizing background photofragmentation. We attempted to avoid saturating the transitions by adjusting the intensity of the first laser pulse so that $\leq$5% of the ions were dissociated. After 480 ms the ions were ejected from the QIT into a linear time-of-flight (ToF) mass spectrometer (length 0.9 m). Electronic spectra were obtained by plotting the charged photofragment signal as a function of wavelength with intensities normalised by OPO power. Wavelength calibration was accomplished with a wavemeter (High Finesse, LSA).

Geometries of C_{2n}^+ clusters were optimised using density functional theory, employing the range separated CAM-B3LYP functional[35] with the cc-pVDZ basis set[36] and empirical dispersion (D3BJ)[37] using Gaussian16.[38] As shown in Section S1 of the SI, the dissociation energies and ionization energies of the carbon clusters calculated using the CAM-B3LYP-D3(BJ)/cc-pVDZ approach compare reasonably well with available experimental data.[39–41] For the C_{11}^+– C_{18}^+ clusters our calculations reproduce the observed variation of dissociation energies with cluster size reported in ref. 39, although the calculated dissociation energies are larger than the experimental dissociation energies by between 5% and 23%. For C_{11}^+–C_{15}^+ clusters our calculations underestimate the experimental ionization energies reported in ref. 40 by between 4% and 17%. The CAM-B3LYP-D3(BJ)/cc-pVDZ method yields

similar dissociation and ionization energies to previous calculations, which employed the B3LYP/def2-TZVPP method,[31] and the high level CCSD(T)/cc-pVQZ method.[40] High level methods such as CCSD(T) are too expensive for the larger carbon clusters targeted in this study. The CAM-B3LYP-D3(BJ)/cc-pVDZ method provides a good compromise between cost and accuracy, and is employed for all investigated carbon species (from C to C_{36}).

Results and Discussion

Electronic spectra of even cyclo[n]carbon cations

The rich and potentially confusing mixture of carbon cluster isomers generated by laser ablation of graphite is illustrated in Figure 2(a), which shows arrival time distributions (ATDs) for even C_{14}^+– C_{36}^+ clusters driven by an electric field through a drift region containing helium buffer gas (signal recorded at detector 1 in Figure 1(c)). The more prominent peaks in the ATDs are due to rings, bi-rings, and fullerenes (single and multiply charged), as observed in previously reported ATDs of carbon cluster cations.[9,11,12] We find that clusters between C_{10}^+ and C_{28}^+ are predominately monocyclic rings and that monocyclic rings persist at least up to C_{40}^+ (see Figure 2(a)). Bi-ring clusters become increasingly apparent from their onset at C_{22}^+ and are more abundant than rings above C_{30}^+ (depending on ion source conditions). Bi-rings are predicted to consist of two rings linked by a four-membered ring, as shown in Figure 1(a).[42] The ATD peaks for bi-rings are broader and more asymmetric than the ring peaks, presumably because carbon atoms can be distributed in different ways between the two rings, giving several bi-ring isomers with different collision cross sections (see Figure 1(a)).[42] Fullerenes first become apparent for C_{28}^+ (very low abundance) and constitute the main isomer for C_{36}^+ and larger clusters.

It is evident from Figure 2(a) that for carbon cluster cations larger than C_{26}^+, there are two or more isomers with comparable abundances (ring, bi-ring, and single and multiply charged fullerenes), and that to avoid isomeric ambiguity it is essential to select the

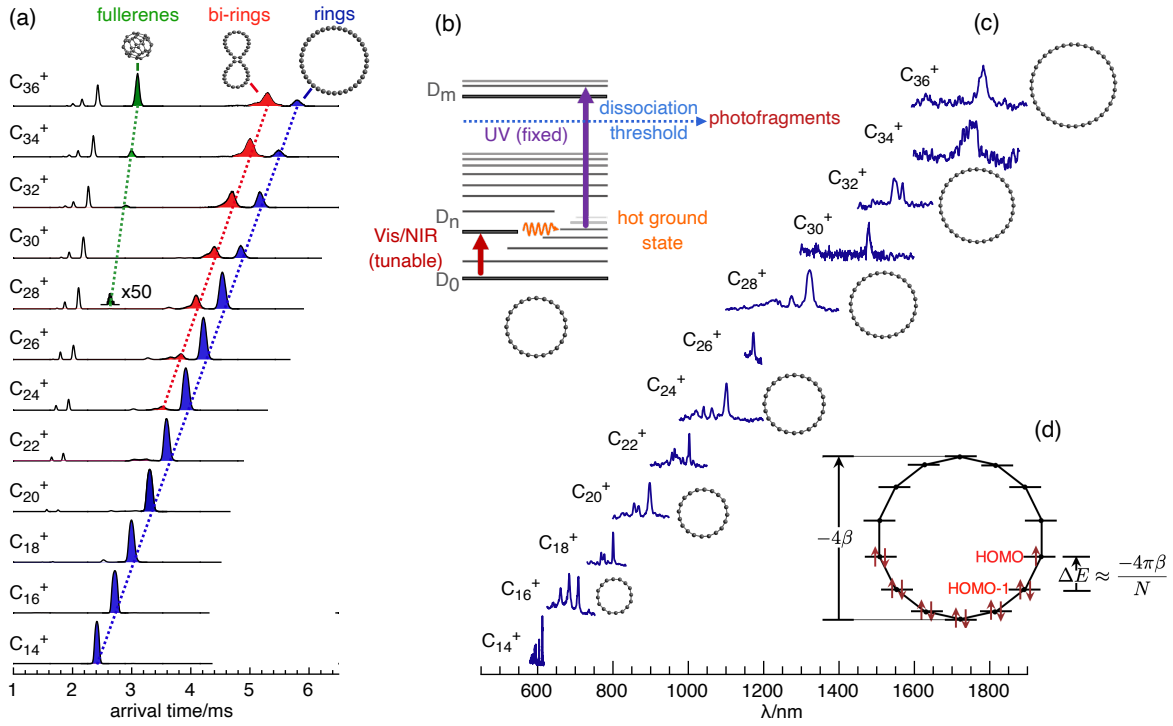

Figure 2: (a) ATDs for carbon cluster cations generated by 532 nm laser ablation of a graphite disk monitoring the ion signal at detector 1 (see Figure 1(c)). Peaks due to rings, bi-rings and fullerenes are highlighted in blue, red and green, respectively. Unlabelled peaks at shorter arrival time are due to larger fullerenes bearing multiple charges. (b) 2-colour resonance enhanced photodissociation scheme for obtaining electronic spectra. (c) Electronic spectra of C_{14}^+–C_{36}^+ rings. The target cyclo[n]carbon clusters (blue peaks in (a)) were mobility-selected following the drift region of the apparatus using the pulsed electrostatic ion gate (see Figure 1(c)) before being probed using the scheme shown in (b). (d) Frost-Musulin diagram showing Hückel energies for in-plane π orbitals of C_{14}^+.

target isomer population *prior* to spectroscopic interrogation. This is accomplished using an electrostatic ion gate at the end of the drift region that is opened at appropriate delay and duration to pass ions with a narrow range of collision cross sections (see Figure 1(c)). These ions subsequently pass through a quadrupole mass filter tuned to the mass of the desired target ion and then into a cryogenically cooled quadrupole ion trap where they are spectroscopically probed using the 2-color resonance enhanced photodissociation (REPD) scheme shown in Figure 2(b). For more details see ref. 26, which describes separation and spectroscopic interrogation of ring and bi-ring isomers of C_{28}^+.

Electronic spectra of isomer-selected even C_{14}^+– C_{36}^+ radical cation rings (blue peaks in Figure 2(a)) are shown in Figure 2(c). Each spectrum shown in Figure 2(c) is the average of 4 or more individual scans. In each case the observed band presumably corresponds to the lowest energy transition with appreciable intensity that proceeds from the doublet ground state to a doublet excited state. As explained below, in a Hückel picture the transition would correspond to promotion of an electron from the HOMO-1 to the HOMO for the in-plane π system (Figure 2(d)). Wavelengths for the main transitions for the C_{2n}^+ clusters are listed in Table 1. The C_{14}^+– C_{28}^+ spectra exhibit similar vibronic structure to the structure observed in previously reported spectra for C_{2n}^+-$(N_2)_m$ and C_{2n}^+-He_m clusters.[24,25] Electronic spectra of C_{30}^+, C_{32}^+, C_{34}^+ and C_{36}^+ clusters (tagged or untagged) have not been reported previously. Comparison of the absorption wavelengths for the C_{2n}^+, C_{2n}^+-$(N_2)_m$ and C_{2n}^+-He_m clusters, show that the spectral shifts caused by He and N_2 tags are relatively small and for the larger clusters (above C_{20}^+) are less than the band widths. Shifts in the transitions of C_{14}^+, the cluster with the sharpest bands, are discussed in more detail below.

A characteristic feature of the cation carbon rings is the regular wavelength shift of the main electronic transition by around 100 nm for each additional two carbon atoms.[24] This trend is illustrated in Figure 3(a), where wavelengths of the transitions are plotted as a function of cluster size. Another obvious aspect of the spectra shown in Figure 2(b) is the alternation of band widths with size – the aromatic C_{4k+2}^+ clusters (C_{14}^+, C_{18}^+ *etc.*) have narrow bands, whereas bands of the anti-aromatic C_{4k}^+ clusters (C_{16}^+, C_{20}^+ *etc.*) are broader. This alternation is apparent in Figure 3(b) where the widths of the origin transitions are plotted as a function of cluster size. Although the bandwidth alternation is quite evident for C_{14}^+ to C_{30}^+, the situation is not so clear for C_{32}^+, C_{34}^+ and C_{36}^+. In particular, the C_{34}^+ peak should be narrow based on the trend for the smaller clusters, but is instead very broad. However, it is worth noting that the C_{34}^+ transition was difficult to obtain, and the transition may be somewhat saturated. The band-width alternation, which is also

Table 1: Measured origin transition wavelengths (nm in air) for bare C_n^+ rings, for previously measured C_n^+-N_2 clusters from ref. 24, for C_n^+-He clusters from ref. 25, and estimated for bare C_n^+clusters from ref. 25.

cluster	C_n^{+a}	C_n^+-$N_2{}^b$	C_n^+-He^c	C_n^{+c} extrapolated
C_{36}^+	1783 ± 10			
C_{34}^+	1747 ± 10			
C_{32}^+	1568.6 ± 3.0			
	1545.6 ± 3.0			
C_{30}^+	1477.6 ± 3.0			
C_{28}^+	1321.6 ± 3.0	1320.6 ± 3.5	1323.4 ± 0.7	1324.3 ± 1
C_{26}^+	1171.8 ± 3.0	1173.1 ± 0.7		
C_{24}^+	1100.1 ± 2.0	1099.3 ± 2.4	1100.5 ± 0.5	1101.2 ± 0.9
C_{22}^+	1002.5 ± 1.0	1001.6 ± 0.5	1002.0 ± 0.5	1002.5 ± 0.6
C_{20}^+	897.5 ± 1.0	898.6 ± 1.6	896.8 ± 0.5	897.2 ± 0.6
C_{18}^+	799.0 ± 1.0	797.5 ± 0.3 ^{d}	799.1 ± 0.5	799.5 ± 0.6
C_{16}^+	709.2 ± 1.0	709.5 ± 1.0	708.6 ± 0.5	708.8 ± 0.5
C_{14}^+	612.7 ± 0.1	611.9 ± 0.2	612.4 ± 0.1	612.6 ± 0.2

^{a} this work. ^{b} ref. 24 ^{c} ref. 25. ^{d} wavelength for C_{28}^+-$(N_2)_2$ transition

apparent in spectra of C_{2n}^+-$(N_2)_m$ and C_{2n}^+-He_m clusters,[24,25] has been hypothesized as due to variations in the rate of non-radiative decay for the clusters[24] – the lowest quartet state, which may be involved in non-radiative deactivation, lies just above the doublet ground state for the anti-aromatic clusters, and somewhat higher in energy for the aromatic clusters.[43] With increasing cluster size, the excited doublet state drops in energy, necessarily reducing the gap with the lower lying quartet state. This may affect the coupling between excited doublet state and the quartet vibronic states for the larger clusters and may mean that isolated resonances play a greater role. For C_{32}^+ there are actually two bands in the origin region spaced by $95\,cm^{-1}$, with the higher energy band being ≈3 times stronger than the lower energy band. The cause of the band doubling is uncertain but may be associated with an interaction between the excited doublet state and another vibronic state (possibly a quartet state). It is also worth pointing out that the transition energies of C_{32}^+, C_{34}^+ and C_{36}^+ are only 0.80, 0.71 and 0.70 eV, respectively, and lie in the energetic vicinity of vibrational

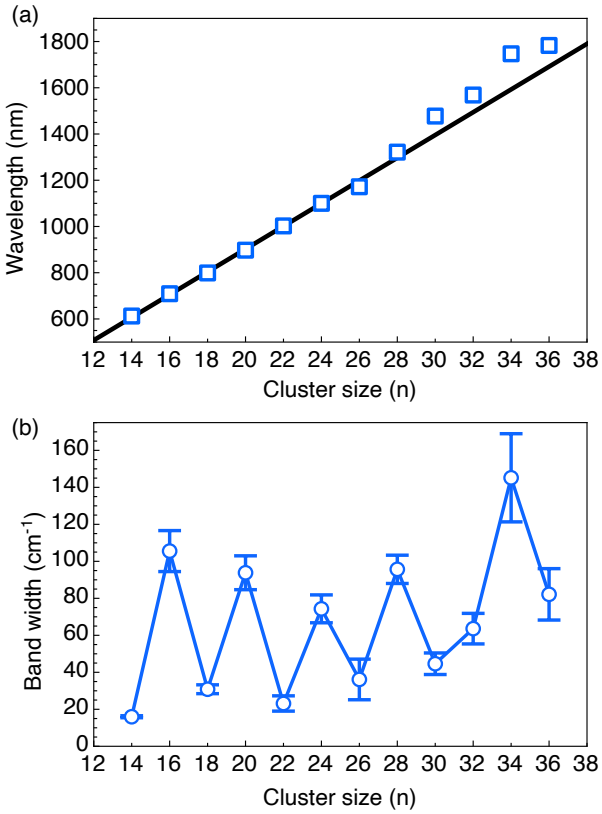

Figure 3: (a) Wavelengths for origin transitions of even cyclo[n]carbon radical cations as a function of n. The linear fit is for C_{14}^+ to C_{28}^+ data. Absorptions of the larger clusters, C_{30}^+ to C_{36}^+, occur to longer wavelength than expected from the linear trend established for the smaller clusters. (b) Widths of origin transitions as a function of cluster size. The plotted widths are based on Gaussian fits to the origin bands with error bars corresponding to twice the standard deviation of fit. There are two peaks in the origin transition region for C_{32}^+ (see Table 1). The width of the broader peak ($64\pm8\,cm^{-1}$) is reported in (b) while the narrower band has a width of $26\pm6\,cm^{-1}$.

levels involving 3 or 4 quanta of highest frequency C-C stretch modes, so resonances with vibrational levels associated with the ground electronic state may also be important.

Hückel model for transition wavelengths of C_{2n}^+ rings

The linear shift of the transitions of the C_{2n}^+ rings with cluster size can be rationalised using a simple Hückel theory model. The cyclo[n]carbons possess an out-of-plane π orbital

system that is antisymmetric with respect to reflection in the molecular plane, and an orthogonal in-plane π orbital system that is symmetric with respect to reflection in the molecular plane (see Figure 1(b)). These two π systems are identical in the limit of an infinitely large ring. However, for finite rings the overlap of the contributing in-plane atomic p orbitals is reduced due to ring curvature, so that each in-plane orbital lies slightly higher in energy than its counterpart out-of-plane orbital.[44] Therefore, in a Hückel framework, the HOMO for the cyclo[n]carbons will be a singly occupied in-plane π orbital (see Figure 2(d)).[45,46] The lowest energy transition not involving promotion from an in-plane to an out-of-plane orbital (or *vice versa*) should correspond to promotion of an electron from the in-plane HOMO-1 orbital to the in-plane HOMO orbital.

Energies, e_j, for the Hückel MOs for a ring of N carbon atoms are given by:[45,46]

$$e_j = \alpha + 2\beta cos(2j\pi/N) \tag{1}$$

with j=0, ±1, ±2, .. , $\pm(\frac{N}{2}-1)$, $\frac{N}{2}$ for N even, and j=0, ±1, ±2, .. , $\pm\frac{N-1}{2}$ for N odd. Here, α is the Coulomb integral and β is the resonance integral. Orbital energies for the cyclo[n]carbons can be represented by Frost-Musulin diagrams as shown in Figure 2(d) for $C_{14}{}^{+}$.[46] The circumscribing circle has a diameter of -4β and the length of the arc between adjacent points is $-4\pi\beta/N$.[46] It can be seen geometrically from Figure 2(d) that, as N increases, the energy difference (ΔE) between the fully occupied HOMO-1 ($e_{(N-2)/4}$) and partially occupied HOMO orbital ($e_{(N-2)/4-1}$) is given approximately by:

$$\Delta E = e_{(N-2)/4} - e_{(N-2)/4-1} \approx -4\pi\beta/N \tag{2}$$

Equation 2 is also derived algebraically from Equation 1 for aromatic and anti-aromatic rings in the Supplementary Information. The wavelength of the lowest energy transition from the

HOMO-1 to the HOMO is then:

$$\lambda_N = hc/\Delta E = -hcN/4\pi\beta \quad (3)$$

showing that the transition wavelengths should shift linearly with N. The difference between the transition wavelengths for the N and $N+2$ rings is:

$$\Delta\lambda = -hc/2\pi\beta \quad (4)$$

Experimentally, $\Delta\lambda$ is ≈100 nm, corresponding to β= –2 eV.

For rings up to C_{28}^+, the crude Hückel model successfully predicts the observed linear trend for the origin wavelengths as a function of cluster size. However, the absorptions of the larger clusters, C_{30}^+ to C_{36}^+, occur to longer wavelength than expected from the linear trend established for the smaller clusters (C_{14}^+ to C_{28}^+). For example, the C_{32}^+, C_{34}^+ and C_{36}^+ bands lie 74, 154 and 92 nm to longer wavelength, respectively, compared to their expected positions based on the linear fit for the smaller clusters' wavelengths (see Figure 3). The origin of the departures from linearity is unclear, but may be associated with a progressive transition to polyynic structures with increasing cluster size.[5,21,23,47] Hot bands are another possible cause for shifting and broadening of the peaks with cluster size. As the rings become larger they should become increasingly floppy, so that even at cryogenic temperatures ($T \approx 10\,K$), low frequency ring deformation vibrational modes should be populated. Distortions from planar, circular structures may affect the electronic energies, such that the hot bands are displaced from the fundamental transitions. The lowest frequency ring deformation modes progressively diminish in frequency with increasing ring size so that hot bands should become more important for larger clusters. For example, DFT CAM-B3LYP-D3(BJ)/cc-pVDZ calculations predict that the four lowest frequency vibrational modes of C_{22}^+ have frequencies of 6, 40, 52, and 52 cm^{-1}, whereas the four lowest frequency modes of C_{36}^+ have frequencies of 5, 15, 20, and 20 cm^{-1}. Given that the QIT temperature is 10 K, one would

expect that only ring distortion vibrational modes with frequencies below ≈20 cm^{-1} will be significantly populated (assuming a Boltzmann distribution). In principle, it should be possible in future experiments to explore the spectral consequences of exciting low frequency ring modes by recording electronic spectra of the clusters with the QIT held at different temperatures.

Spectrum of C_{14}^+- astrophysical implications and effect of tag atoms and molecules

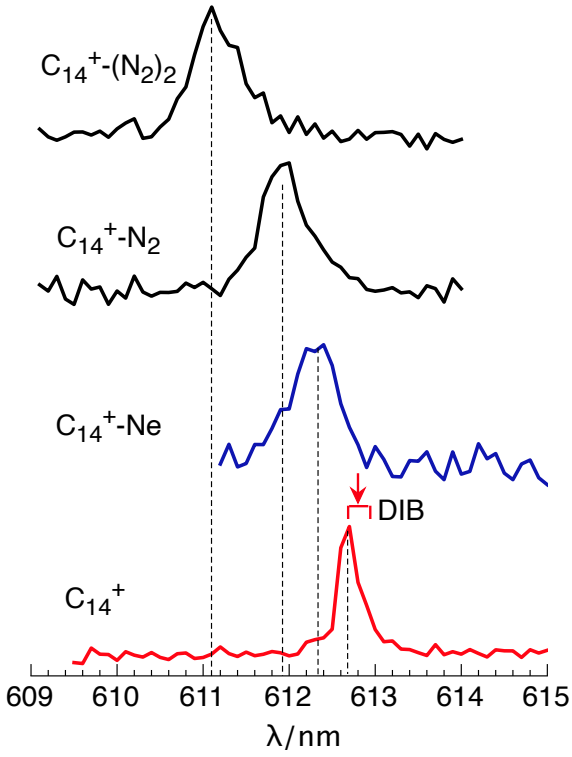

Figure 4: Electronic spectra of C_{14}^+, C_{14}^+-Ne, C_{14}^+-N_2 and C_{14}^+-$(N_2)_2$. Spectra of C_{14}^+-N_2, C_{14}^+-$(N_2)_2$ and C_{14}^+-Ne were recorded by monitoring the photodepletion of the respective complex using 1-colour REPD. The spectrum of bare C_{14}^+ was obtained by 2-colour REPD monitoring C_{11}^+ photofragments. The wavelength and width for the weak 612.820 nm DIB reported in ref. 48 are indicated above the C_{14}^+ plot.

The cyclo[n]carbon cations are possible constituents of interstellar and circumstellar regions and may be detectable through their electronic transitions. Due to its relatively narrow

transitions the C_{14}^+ ring is perhaps the best candidate for detection. As noted previously,[24,25] the relatively sharp C_{14}^+ absorption lies close to a weak diffuse interstellar band (DIB) at 612.820 nm with a width of 0.218 nm.[48] The current measurements confirm that the maximum of the origin band for bare C_{14}^+ is displaced by only 0.1 nm from the weak DIB (see Figure 4). The rotational temperature of the trapped C_{14}^+ ions (10 K) is likely lower than for molecules in the interstellar medium (50–80 K), so that comparisons between astronomical and laboratory data requires spectra of bare C_{14}^+ clusters for elevated ion trap temperatures to track the evolution of the band maximum and band contour with temperature.[25] If C_{14}^+ is indeed a DIB carrier, weaker peaks lying to shorter wavelengths at 604.2 nm ($\approx \times 0.5$ the intensity of the 612.7 nm band) and at 602.9 nm ($\approx \times 0.2$ the intensity of the 612.7 nm band), should also correspond to weak DIBs. Currently there are no appropriate matches for these peaks in published spectra of HD183143 or HD204827,[48,49] although the signal-to-noise ratio of astronomical spectra in the appropriate wavelength range may need to be improved for their detection.

Previous spectra of the cyclo[n]carbon cations were recorded by forming and photodissociating weakly-bound complexes of the target cyclo[n]carbon cation tagged with He atoms[25] or N_2 molecules.[24] The band displacements caused by the tag atoms and molecules are clearly apparent in the spectra for C_{14}^+, C_{14}^+-Ne, C_{14}^+-N_2 and C_{14}^+-$(N_2)_2$ shown in Figure 4. The band maximum for the bare C_{14}^+ ring lies at 612.7±0.1 nm, close to the wavelength (612.6 nm) deduced by Campbell *et al.* from C_{14}^+-He and C_{14}^+-He_2 spectra, assuming that the spectral shifts caused by the first and second He atoms are additive.[25] Addition of He or Ne atoms shifts the C_{14}^+ origin transition to higher energy by ≈8 and ≈11 cm^{-1}, respectively. The shifts caused by N_2 molecules are larger (+21 cm^{-1}/N_2 molecule) and additive, consistent with structures in which the first two N_2 molecules occupy equivalent sites above and below the C_{14}^+ ring.[24] The conclusion is that spectral shifts caused by He, Ne and N_2 tags are relatively small, but are significant when transition wavelengths are to be compared with astronomical data.

Photodestruction of colossal carbon rings

We turn now to consider the photodestruction of cyclo[n]carbon radical cations. From previous investigations, it is known that charged fullerene carbon clusters decompose mainly through loss of C_2 molecules,[29] whereas smaller clusters with $n \leq 20$ tend to lose C_3 or C_5 molecules.[27,28,30,31] In the intermediate size range $20 \leq n \leq 40$ the photofragment distributions have been found to be sensitive to ion source conditions and laser power, suggesting that the cluster population contained different isomers, each with distinct absorption cross section and photodissociation behaviour.[29] Here we focus on even carbon rings (C_{14}^+ to C_{36}^+), and remove any structural ambiguity by selecting and probing only the ring isomer for each cluster size. Isomer selection is particularly important for the larger clusters. For example, for C_{30}^+ the ring and bi-ring isomers have relative populations of 1:1, while for C_{36}^+ the ring, bi-ring and fullerene isomers have relative populations of 1:3:3. We attempted to control the energy delivered to the clusters by using a two-photon resonance-enhanced excitation scheme (Figure 5a), whereby a relatively low power pulse of visible/NIR light ($\leq$1 mJ/cm^2/pulse) tuned to the origin transition of the ring under examination was followed 10 ns later by a pulse of 230 nm UV light ($\leq$1 mJ/cm^2/pulse). Intensities of the two beams were adjusted to limit the photodissociated fraction to $\leq$10% to reduce the effects of consecutive photon absorption. Assuming the clusters absorb one visible/NIR photon and one 230 nm photon, the total energy delivered to the clusters is 6.1–7.4 eV (the lower limit corresponds to C_{36}^+ and the upper limit to C_{14}^+). This energy should suffice to break the clusters into two fragments, but be insufficient to cause sequential fragmentation.[39] Photofragmentation mass spectra obtained under these conditions are shown in Figure 5b. The smaller clusters, up to C_{22}^+, tend to lose either a C_3 or C_5 unit, as observed in previous studies.[27,30,31] Rings larger than C_{26}^+ also lose C_3 or C_5 units, but additionally produce C_{14}^+, C_{18}^+, and C_{22}^+ photofragments. These preferred larger cluster fragments would, if they were cyclic, have aromatic stability. To help understand the photofragment distributions apparent in Figure 5b, we calculated relative energies for different photofragment combinations. These

energies are plotted in Figure 5c where it can be seen that the lower energy fragmentation channels correspond to the preferred photofragments apparent in Figure 5b. On energetic grounds, rings in the C_{28}^+– C_{36}^+ size range can be expected to break up into two smaller rings, one neutral and one charged, consistent with the photofragment mass spectra shown in Figure 5b. Similar fragmentation patterns are found for cyclo[n]carbon cations subjected to collisional activation.[10,11,50]

To investigate whether the larger charged photofragments are indeed cyclo[n]carbons, we irradiated selected C_{28}^+ rings in the QIT with a pulse of 235 nm light early in the trapping cycle to form photofragments that were subsequently tagged with N_2 molecules (the trap gas for these experiments was a 1% N_2/He mixture) and recorded their electronic spectra with 1-colour REPD. As an example, REPD spectra of N_2-tagged C_{14}^+ and C_{18}^+ clusters formed by photodissociating C_{28}^+ ions in the QIT, are shown in Figure 6(a). The C_{14}^+ and C_{18}^+ photofragment spectra are identical to the spectra of C_{14}^+ and C_{18}^+ produced directly by the laser ablation ion source,[24] proving that large C_{2n}^+ rings predominately photodissociate to give smaller rings. Although, we have no information on the neutral co-fragments, they are almost certainly rings as the linear isomers lie much higher in energy.

We hypothesise that rupture of a large ring to generate two smaller rings follows a process whereby electronic excitation is followed by internal conversion to give a vibrationally energized cluster which distorts and twists to form a bicyclic cluster that subsequently breaks into two smaller rings. Key steps along this pathway, calculated at the DFT CAM-B3LYP-D3(BJ)/cc-pVDZ level, are shown in Figure 6 for C_{28}^+ disintegrating to $C_{14}^+ + C_{14}$ ring fragments. In this case, the $C_{14}^+ + C_{14}$ and $C_{18}^+ + C_{10}$ fragment channels have similar energies, consistent with the observation of strong C_{14}^+ and C_{18}^+ signals in the C_{28}^+ photofragment mass spectrum (Figure 5b).

Equipped with the distinctive electronic spectra for C_{2n}^+ rings, we are in a position to assess the structures of the carbon cluster photofragments from other molecular systems, including charged PAHs, which upon exposure to light in ion traps, undergo progressive

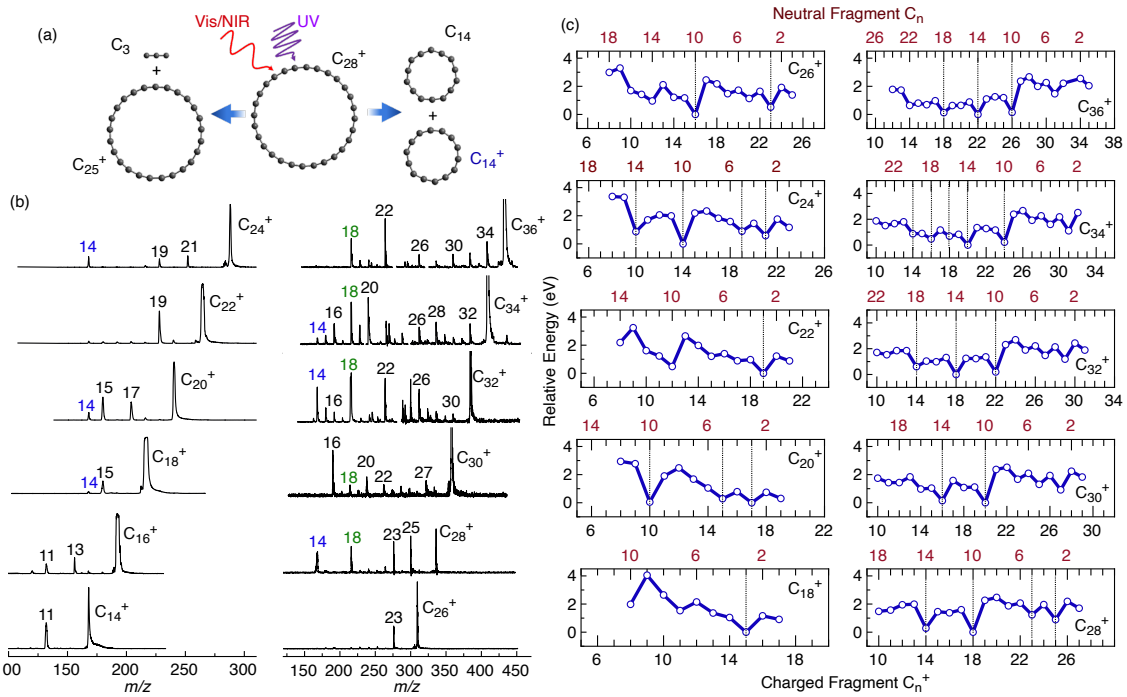

Figure 5: (a) Example of the two most significant photodissociation pathways for carbon rings in the C_{14}^+ to C_{36}^+ range: loss of neutral C_3 or C_5 molecules, and fragmentation to two rings, one neutral and one charged. (b) Photofragment mass spectra for isomer-selected C_{14}^+ to C_{36}^+ cyclo[n]carbons. The clusters were energised through resonance-enhanced two-photon excitation, with the first photon tuned to the cluster's main Vis/NIR transition ($\leq$1 mJ/cm^2/pulse) and wavelength of the second photon fixed at 230 nm ($\leq$1 mJ/cm^2/pulse). The numbers above the peaks indicate the number of carbon atoms in the photofragment cations. Loss of C_3 and C_5 neutrals for smaller clusters is augmented by loss of C_{10}, C_{14} and C_{18} for larger clusters. Photofragment ToF mass spectra for the larger clusters were recorded in sections so that relative peak intensities are indicative rather than quantitative. (c) Relative energies for pairs of fragments from C_{2n}^+(n=9–18) cyclic clusters calculated at the CAM-B3LYP-D3(BJ)/cc-pVDZ level. Fragments smaller than C_{10}^+ are linear, whereas larger fragments are cyclic. Energies for fragment pairs involving fullerenes, which may be important for C_{32}^+, C_{34}^+ and C_{36}^+, are not shown in the plot. The more stable product pairs are indicated by dotted vertical lines. Fragment energies are given in Table S1 in the SI.

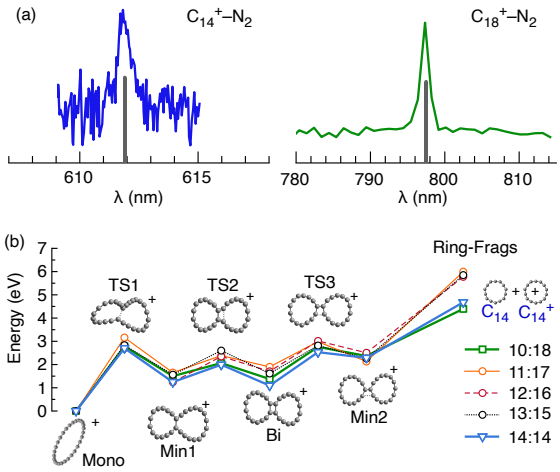

Figure 6: (a) Electronic spectra of C_{14}^+-N_2 and C_{18}^+-N_2 clusters that were generated by photodissociating C_{28}^+ in the cryogenic ion trap to form C_{14}^+ and C_{18}^+ ions that were subsequently tagged with N_2 molecules. The spectrum on the left was obtained by monitoring photodepletion of C_{14}^+-N_2, and the spectrum on the right by monitoring formation C_{18}^+ from C_{18}^+-N_2. Vertical lines indicate transition wavelengths for C_{14}^+-N_2 and C_{18}^+-N_2 reported in ref. 24. (b) Structures on the path for dissociation of the C_{28}^+ ring to give a pair of cyclic fragments. Structures and energies are calculated at the DFT CAM-B3LYP-D3(BJ)/cc-pVDZ level.

dehydrogenation to yield charged carbon clusters.[15,16] The chemical fate of PAHs subject to UV radiation is a crucial issue in regions of the interstellar medium.[51] The question is whether product carbon clusters, which include C_{14}^+ and C_{18}^+, retain the structure of the PAH skeleton or whether they rearrange to become cyclo[n]carbons, or perhaps some other low energy isomer.

Notably, the C_{34}^+ and C_{36}^+ rings also have a propensity for losing C_2 units (see Figure 5), as does C_{32}^+ to a lesser extent. The loss of C_2 is a characteristic feature for the breakup of fullerenes induced by collisions or photon absorption,[29,52–54] but is less usual for C_n^+ rings. Remembering that the photofragmentation mass spectra shown in Figure 5 were obtained for isomer-selected cyclo[n]carbon cations, this raises the intriguing possibility that photo-excitation triggers a transformation of C_{34}^+ and C_{36}^+ rings to fullerenes with concomitant C_2 loss(es) (and perhaps C_4 and C_6 losses). The process is akin to the transformation of planar rings to fullerenes that was deduced to occur when rings were subjected to energetic collisions

prior to analysis in an ion mobility spectrometer.[52,53] Exothermicities for conversion of rings to fullerenes + C_2 are predicted to be substantial. For example, using calculated energies given in Table S1 in the SI, the C_{36}^+(ring)→C_{34}^+(fullerene) + C_2 reaction is predicted to be exothermic by 6.3 eV. In contrast, the C_{36}^+(ring)→C_{34}^+(ring) + C_2 pathway is endothermic by 6.5 eV, and is probably less likely to occur.

As a test, we also exposed isomer-selected C_{36}^+ fullerene clusters to pulses of 235 nm light and found that they strongly resisted photofragmentation compared to the ring isomers, consistent with the high C_2 binding energy (calculated to be 10.2 eV for the C_{36}^+ fullerene), and agreeing with previous observations that photodecomposition of fullerenes requires very high light intensities compared to other isomers.[29]

Conclusions

The current work demonstrates the power of gas-phase spectroscopy for elucidating the properties of cyclo[n]carbon clusters. The outcomes of the work can be summarised as follows.

1. Electronic spectra of untagged, isomer-selected carbon cluster cations from C_{14}^+ to C_{36}^+ are obtained through two-colour action spectroscopy. Tag-free spectra of the carbon cluster cations are essential for comparisons with astronomical data and to judge the effects of attached tag atoms or molecules, which are not known *a priori*. The possibility of detecting C_{14}^+ in the interstellar medium is considered. The origin transition of bare C_{14}^+ at 612.7 nm lies 0.1 nm from a weak diffuse interstellar band at 612.82 nm. Further, spectroscopic studies are required to explore the effect of temperature on the band's position and shape. We present the first electronic spectra of C_{30}^+, C_{32}^+, C_{34}^+, and C_{36}^+ cyclo[n]carbon cations. Despite C_{34}^+ and C_{36}^+ rings being far less stable than the fullerene isomers, by performing isomer-selective spectroscopy, we show that they survive at least $\approx 10^6$ collisions with helium atoms at room temperature, and can be isolated and stored for relatively long periods of time (at least 1 s) in a cryogenic ion trap.

2. We have developed a simple Hückel theory model to explain the linear shift of the wavelengths for the C_{2n}^+ absorption bands with cluster size. The model works well for clusters up to C_{28}^+, but begins to break down for larger clusters, perhaps due their increased floppiness, which may mean that they explore distorted geometries, even at cryogenic temperatures.

3. Photofragmentation distributions are measured for isomer-selected carbon ring cations. Isomer selection is particularly important for clusters containing more than 20 carbon atoms, for which there are several isomers, each of which should have a characteristic photofragment distribution. Smaller rings decompose by losing C_3 and C_5 molecules, while larger rings (C_{24}^+ and larger), also break up into neutral and charged rings. The observed dissociation channels generally correspond to production of fragment pairs that are predicted through DFT calculations to lie lower in energy.

4. To explore the photodecomposition of larger carbon rings, we trapped isomer-selected C_{28}^+ rings, exposed them to radiation, and then measured the electronic spectra of C_{14}^+ and C_{18}^+ photofragments tagged with N_2 molecules, confirming that these fragments are also rings. We proposed a mechanism for the fission of cyclic C_{28}^+ based on DFT calculations, in which the penultimate fragmentation steps involve a bi-ring intermediate.

5. Photoexcitation of C_{34}^+ and C_{36}^+ cyclo[n]carbon isomers lead to loss of neutral C_2 units, which may indicate that C_{34}^+ and C_{36}^+ cyclo[n]carbons photoisomerise into fullerenes before dissociation. In principle, this transformation could be explored using a tandem ion mobility mass spectrometer (IMS), with photo-excitation of selected rings following the first IMS stage and separation of photoproduct isomers in the second IMS stage, as described in ref. 33. Photoconversion of carbon rings to fullerenes may be an important process in regions of the interstellar medium where stellar ultraviolet radiation is ubiquitous but where energetic collisions are infrequent due to low densities and temperatures.[55]

There are several avenues for further work. Given that rings as large as C_{80}^+ have been observed in ion mobility studies,[13] it would be interesting to continue spectroscopic studies to rings larger than C_{36}^+, following the trajectory of the band system further into the infrared

where eventually it should have a similar energy to the ring's vibrational spacings. More structural information on the rings could also be derived from infrared spectra, particularly regarding the transition from cumulenic bonding in smaller cyclo[n]carbons with equal C-C bond lengths to polyynic structures for larger clusters possessing alternating single and triple bonds.[5,21,23,47] Future spectroscopic studies will undoubtedly also target odd cyclo[n]carbon cations ($C_{2n+1}{}^+$).

Supporting Information Available

Supporting Information contains: (i) calculated ground state energies for cation and neutral carbon clusters, (ii) calculated dissociation energies of $C_n{}^+$ clusters, (iii) calculated ionisation energies of C_n clusters, (iv) an analytical derivation of the Hückel theory model, and (v) xyz coordinates for calculated equilibrium geometries of C_n and $C_n{}^+$ clusters.

Acknowledgement

This research was supported under the Australian Research Council's Discovery Project funding scheme (Project Numbers DP150101427 and DP160100474). U. J. acknowledges support from the Swiss National Science Foundation (P2EZP2_178429). We thank Richard Mathys of the Science Faculty Workshop and Luke Weston for indispensable contributions to the design and construction of the apparatus. We thank Dr. Ewen Campbell for helpful discussions.

Conflict of Interest

The authors have no conflicts to disclose.

Data Availability Statement

The data that support the findings of this study are available from the corresponding author upon reasonable request.

References

(1) Kroto, H. W.; Heath, J. R.; O'Brien, S. C.; Curl, R. F.; Smalley, R. E. C_{60}: Buckminsterfullerene. *Nature* **1985**, *318*, 162–163.

(2) Weltner, W.; Van Zee, R. J. Carbon molecules, ions, and clusters. *Chem. Rev.* **1989**, *89*, 1713–1747.

(3) Van Orden, A.; Saykally, R. J. Small carbon clusters: Spectroscopy, structure, and energetics. *Chem. Rev.* **1998**, *98*, 2313–2357.

(4) Pitzer, K. S.; Clementi, E. Large molecules in carbon vapor. *J. Am. Chem. Soc.* **1959**, *81*, 4477–4485.

(5) Anderson, H. L.; Patrick, C. W.; Scriven, L. M.; Woltering, S. L. A short history of cyclocarbons. *Bull. Chem. Soc. Jpn.* **2021**, *94*, 798–811.

(6) Hahn, O.; Strassmann, F.; Mattauch, J.; Ewald, H. Hat in früheren Erdperioden ein radioaktives Cäsium existiert? Barium und Strontium aus Pollucit. *Naturwissenschaften* **1942**, *30*, 541–542.

(7) McElvany, S. W.; Creasy, W. R.; O'Keefe, A. Ion–molecule reaction studies of mass selected carbon cluster ions formed by laser vaporization. *J. Chem. Phys.* **1986**, *85*, 632–633.

(8) McElvany, S. W.; Dunlap, B. I.; O'Keefe, A. Ion molecule reactions of carbon cluster ions with D_2 and O_2. *J. Chem. Phys.* **1987**, *86*, 715–725.

(9) von Helden, G.; Hsu, M.; Kemper, P. R.; Bowers, M. T. Structures of carbon cluster ions from 3 to 60 atoms: Linears to rings to fullerenes. *J. Chem. Phys.* **1991**, *95*, 3835–3837.

(10) von Helden, G.; Gotts, N. G.; Bowers, M. T. Annealing of carbon cluster cations: rings to rings and rings to fullerenes. *J. Am. Chem. Soc.* **1993**, *115*, 4363–4364.

(11) Hunter, J. M.; Fye, J. L.; Jarrold, M. F. Annealing and dissociation of carbon rings. *J. Chem. Phys.* **1993**, *99*, 1785–1795.

(12) von Helden, G.; Hsu, M. T.; Gotts, N.; Bowers, M. T. Carbon cluster cations with up to 84 atoms: Structures, formation mechanism, and reactivity. *J. Phys. Chem.* **1993**, *97*, 8182–8192.

(13) Hunter, J. M.; Fye, J. L.; Roskamp, E. J.; Jarrold, M. F. Annealing carbon cluster ions: A mechanism for fullerene synthesis. *J. Phys. Chem.* **1994**, *98*, 1810–1818.

(14) Lifshitz, C.; Peres, T.; Agranat, I. Properties of carbon cluster ions, C_n^+, formed by dissociative ionization. *Int. J. Mass. Spectrom. Ion Proc.* **1989**, *93*, 149–163.

(15) Ekern, S. P.; Marshall, A. G.; Szczepanski, J.; Vala, M. Photodissociation of gas-phase polycylic aromatic hydrocarbon cations. *J. Phys. Chem. A* **1998**, *102*, 3498–3504.

(16) West, B.; Useli-Bacchitta, F.; Sabbah, H.; Blanchet, V.; Bodi, A.; Mayer, P. M.; Joblin, C. Photodissociation of pyrene cations: Structure and energetics from $C_{16}H_{10}^+$ to C_{14}^+ and almost everything in between. *J. Phys. Chem. A* **2014**, *118*, 7824–7831.

(17) Hrodmarsson, H. R.; Bouwman, J.; Tielens, A. G. G. M.; Linnartz, H. Similarities and dissimilarities in the fragmentation of polycyclic aromatic hydrocarbon cations: A case study involving three dibenzopyrene isomers. *Int. J. Mass Spectrom.* **2022**, *476*, 116834.

(18) Diederich, F.; Rubin, Y.; Knobler, C. B.; Whetten, R. L.; Schriver, K. E.; Houk, K. N.; Li, Y. All-carbon molecules: Evidence for the generation of cyclo[18]carbon from a stable organic precursor. *Science* **1989**, *245*, 1088–1090.

(19) Kaiser, K.; Scriven, L.; Schulz, F.; Gawel, P.; Gross, L.; Anderson, H. An sp-hybridized molecular carbon allotrope, cyclo[18]carbon. *Science* **2019**, *365*, 1299–1301.

(20) Xu, S.; Liu, F.; Xu, J.; Cui, Y.; Wang, C. Theoretical investigation on bond and spectrum of cyclo[18] carbon (C_{18}) with sp-hybridized. *J. Mol. Model.* **2020**, *26*, 111.

(21) Pereira, Z. S.; da Silva, E. Z. Spontaneous symmetry breaking in cyclo[18]carbon. *J. Phys. Chem. A* **2020**, *124*, 1152–1157.

(22) Hong, I.; Ahn, J.; Shin, H.; Bae, H.; Lee, H.; Benali, A.; Kwon, Y. Competition between Hückel's rule and Jahn-Teller distortion in small carbon rings: A quantum Monte Carlo study. *J. Phys. Chem. A* **2020**, *124*, 3636–3640.

(23) Baryshnikov, G. V.; Valiev, R. R.; Nasibullin, R. T.; Sundholm, D.; Kurten, T.; Ågren, H. Aromaticity of even-number cyclo[n]carbons (n=6–100). *J. Phys. Chem. A* **2020**, *124*, 10849–10855.

(24) Buntine, J. T.; Cotter, M. I.; Jacovella, U.; Liu, C.; Watkins, P.; Carrascosa, E.; Bull, J. N.; Weston, L.; Muller, G.; Scholz, M. S. et al. Electronic spectra of positively charged carbon clusters - C_{2n}^+ (n=6-14). *J. Chem. Phys.* **2021**, *155*, 214302.

(25) Rademacher, J.; Reedy, E. S.; Campbell, E. K. Electronic spectroscopy of monocyclic carbon ring cations for astrochemical consideration. *J. Phys. Chem. A* **2022**, *126*, 2127–2133.

(26) Buntine, J. T.; Carrascosa, E.; Bull, J. N.; Jacovella, U.; Cotter, M. I.; Watkins, P.; Liu, C.; Scholz, M. S.; Adamson, B. D.; Marlton, S. J. P. et al. An ion mobility

mass spectrometer coupled with a cryogenic ion trap for recording electronic spectra of charged, isomer-selected clusters. *Rev. Sci. Instr.* **2022**, *93*, 043201.

(27) Geusic, M. E.; McIlrath, T. J.; Jarrold, M. F.; Bloomfield, L. A.; Freeman, R. R.; Brown, W. L. Photofragmentation of mass-resolved carbon cluster ions: Observation of a "magic" neutral fragment. *J. Chem. Phys.* **1986**, *84*, 2421–2422.

(28) Geusic, M. E.; Jarrold, M. F.; McIlrath, T. J.; Freeman, R. R.; Brown, W. L. Photodissociation of carbon cluster cations. *J. Chem. Phys.* **1987**, *86*, 3862–3869.

(29) O'Brien, S. C.; Heath, J. R.; Curl, R. F.; Smalley, R. E. Photophysics of buckminsterfullerene and other carbon cluster ions. *J. Chem. Phys.* **1988**, *88*, 220–230.

(30) Pozniak, B. P.; Dunbar, R. C. Photodissociation studies of C_n^+ at 193 nm (n = 5-19). *Int. J. Mass. Spectrom. Ion Proc.* **1997**, *165*, 299–313.

(31) Dynak, N. J.; Rittgers, B. M.; Colley, J. E.; Kellar, D. J.; Duncan, M. A. Photofragment imaging of carbon cluster cations: Explosive ring rupture. *J. Phys. Chem. Lett.* **2022**, *13*, 4786–4793.

(32) Moriyama, R.; Ohtaki, T.; Hosoya, J.; Koyasu, K.; Misaizu, F. Isomer-separated photodissociation of large sized silicon and carbon cluster ions: Drift tube experiment combined with a tandem reflectron mass spectrometer for Si_{24}^+ - Si_{27}^+ and C_{32}^+-C_{38}^+. *Eur. Phys. J. D* **2013**, *67*, 1446–5.

(33) Adamson, B. D.; Coughlan, N. J. A.; Markworth, P. B.; Continetti, R. E.; Bieske, E. J. An ion mobility mass spectrometer for investigating photoisomerization and photodissociation of molecular ions. *Rev. Sci. Instr.* **2014**, *85*, 123109.

(34) Marlton, S. J. P.; Buntine, J. T.; Liu, C.; Watkins, P.; Jacovella, U.; Carrascosa, E.; Bull, J. N.; Bieske, E. J. Disentangling electronic spectra of linear and cyclic hydro-

genated carbon cluster cations, $C_{2n+1}H^+$ (n = 3–10). *J. Phys. Chem. A* **2022**, *126*, 6678–6685.

(35) Yanai, T.; Tew, D. P.; Handy, N. C. A new hybrid exchange–correlation functional using the Coulomb-attenuating method (CAM-B3LYP). *Chem. Phys. Lett.* **2004**, *393*, 51–57.

(36) T. H. Dunning, Jr., Gaussian basis sets for use in correlated molecular calculations. I. The atoms boron through neon and hydrogen. *J. Chem. Phys.* **1989**, *90*, 1007.

(37) Grimme, S.; Ehrlich, S.; Goerigk, L. Effect of the damping function in dispersion corrected density functional theory. *J. Comput. Chem.* **2011**, *32*, 1456–1465.

(38) Frisch, M. J.; Trucks, G. W.; Schlegel, H. B.; Scuseria, G. E.; Robb, M. A.; Cheeseman, J. R.; Scalmani, G.; Barone, V.; Petersson, G. A.; Nakatsuji, H. et al. *Gaussian 16*, Revision C.01. Gaussian Inc.: Wallingford, CT, 2016.

(39) Sowa-Resat, M. B.; Hintz, P. A.; Anderson, S. L. Dissociation energies for small carbon cluster ions (C^+_{2-19}) measured by collision-induced dissociation. *J. Phys. Chem.* **1995**, *99*, 10736–10741.

(40) Belau, L.; Wheeler, S. E.; Ticknor, B. W.; Ahmed, M.; Leone, S. R.; Allen, W. D.; Schaefer, H. F.; Duncan, M. A. Ionization thresholds of small carbon clusters: Tunable VUV experiments and theory. *J. Am. Chem. Soc.* **2007**, *129*, 10229–10243.

(41) Harper, O. J.; Boyé-Péronne, S.; Garcia, G. A.; Hrodmarsson, H. R.; Loison, J.-C.; Gans, B. To see C_2: Single-photon ionization of the dicarbon molecule. *J. Chem. Phys.* **2020**, *152*, 041105.

(42) Helden, G. v.; Hsu, M.; Gotts, N.; Kemper, P.; Bowers, M. Do small fullerenes exist only on the computer? Experimental results on $C_{20}{}^{+/-}$ and $C_{24}{}^{+/-}$. *Chem. Phys. Lett.* **1993**, *204*, 15–22.

(43) Giuffreda, M. G.; Deleuze, M. S.; François, J. P. Structural, rotational, vibrational, and electronic properties of ionized carbon clusters C_n^+ (n= 4-19). *J. Phys. Chem. A* **1999**, *103*, 5137–5151.

(44) Fowler, P. W.; Mizoguchi, N.; Bean, D. E.; Havenith, R. W. A. Double aromaticity and ring currents in all-carbon rings. *Chem. Eur. J.* **2009**, *15*, 6964–6972.

(45) Hückel, E. Quantentheoretische beiträge zum problem der aromatischen und ungesättigten verbindungen. III. *Z. Phys.* **1932**, *76*, 628–648.

(46) Frost, A. A.; Musulin, B. A mnemonic device for molecular orbital energies. *J. Chem. Phys.* **1953**, *21*, 572–573.

(47) Parasuk, V.; Almlöf, J.; Feyereisen, M. W. The [18] all-carbon molecule: cumulene or polyacetylene? *J. Am. Chem. Soc.* **1991**, *113*, 1049–1050.

(48) Hobbs, L. M.; York, D. G.; Thorburn, J. A.; Snow, T. P.; Bishof, M.; Friedman, S. D.; McCall, B. J.; Oka, T.; Rachford, B.; Sonnentrucker, P. et al. Studies of the diffuse interstellar bands. III. HD 183143. *Astrophys. J.* **2009**, *705*, 32.

(49) Hobbs, L. M.; York, D. G.; Snow, T. P.; Oka, T.; Thorburn, J. A.; Bishof, M.; Friedman, S. D.; McCall, B. J.; Rachford, B.; Sonnentrucker, P. A catalog of diffuse interstellar bands in the spectrum of HD 204827. *Astrophys. J.* **2008**, *680*, 1256.

(50) Shelimov, K. B.; Hunter, J. M.; Jarrold, M. F. Small carbon rings: Dissociation, isomerization, and a simple model based on strain. *Int. J. Mass. Spectrom. Ion Proc.* **1994**, *138*, 17–31.

(51) Tielens, A. G. G. M. Interstellar polycyclic aromatic hydrocarbon molecules. *Annu. Rev. Astron. Astrophys.* **2008**, *46*, 289–337.

(52) von Helden, G.; Gotts, N. G.; Bowers, M. T. Experimental evidence for the formation

of fullerenes by collisional heating of carbon rings in the gas phase. *Nature* **1993**, *363*, 60–63.

(53) von Helden, G.; Gotts, N. G.; Bowers, M. T. Annealing of carbon cluster cations: rings to rings and rings to fullerenes. *J. Am. Chem. Soc.* **1993**, *115*, 4363–4364.

(54) Zhen, J.; Castellanos, P.; Paardekooper, D. M.; Linnartz, H.; Tielens, A. G. G. M. Laboratory formation of fullerenes from PAHS: Top-down interstellar chemistry. *Astrophys. J. Lett.* **2014**, *797*, L30.

(55) Tielens, A. G. G. M. *The physics and chemistry of the interstellar medium*; Cambridge University Press: Cambridge, 2005.

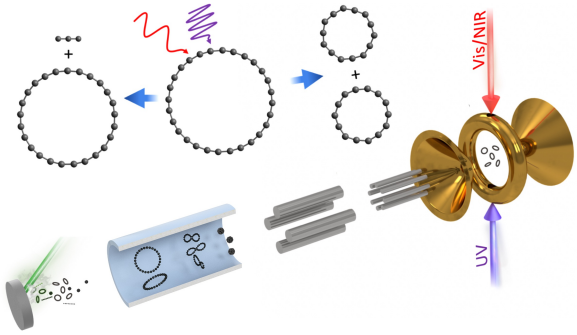

TOC graphic